JOURNAL OF ENERGY, MATERIALS, AND INSTRUMENTATION TECHNOLOGY

Journal Webpage https://jemit.fmipa.unila.ac.id/

Improvement of TiO_2 Performance with 10% Cu–TiO_2/$BiVO_4$ Heterojunction Composite Using Sonication in Photoelectrochemical Water Splitting

Bunga Nurkhalifah*, Vera Pangni Fahriani, Sarah Dampang, Muhammad Fahmi Hakim, and Siti Nurhayati

Chemical Engineering Study Program, Singaperbangsa University Karawang, Indonesia, 41361

Article Information

Article history:
Received August 1, 2025
Received in revised form September 22, 2025
Accepted September 30, 2025

Keywords: *Heterojunction, Photoelectrochemistry, TiO_2, Water splitting*

Abstract

The global energy crisis, driven by the depletion of fossil fuels, has accelerated the search for renewable energy solutions, including hydrogen production via solar-driven photoelectrochemical (PEC) systems. A major limitation of PEC is the UV-only activity of semiconductors such as TiO_2. This study investigates the performance enhancement of TiO_2 through the formation of a Cu–TiO_2/$BiVO_4$ heterojunction composite with 10% Cu doping and sonication treatment. Cu doping reduces the band gap and extends light absorption into the visible region, while $BiVO_4$ promotes effective charge separation. SEM-EDS analysis revealed a more uniform particle distribution in the sonicated sample, and UV-Vis DRS confirmed a substantial band gap narrowing from 2.97 eV to 2.02 eV. PEC testing in a 0.5 M NaCl solution showed that the sonicated composite achieved the highest and most stable photovoltage (0.78 V) along with visible hydrogen bubble formation, indicating efficient light-to-hydrogen conversion. These findings demonstrate that sonication plays a crucial role in improving particle dispersion, suppressing agglomeration, and reinforcing the TiO_2/$BiVO_4$ heterojunction, highlighting its potential as a self-biased photoanode for sustainable hydrogen production.

Informasi Artikel

Proses artikel:
Diterima 1 Agustus 2025
Diterima dan direvisi dari 22 September 2025
Accepted 30 September 2025

Kata kunci:
Heterojunction, Fotoelektrokimia, TiO_2, Pemisahan air

Abstrak

Krisis energi global yang didorong oleh menipisnya bahan bakar fosil telah mempercepat pencarian solusi energi terbarukan, termasuk produksi hidrogen melalui sistem fotoelektrokimia (PEC) bertenaga surya. Keterbatasan utama PEC adalah aktivitas semikonduktor seperti TiO_2 yang hanya bersifat UV. Studi ini menyelidiki peningkatan kinerja TiO_2 melalui pembentukan komposit heterojunction Cu–TiO_2/$BiVO_4$ dengan doping Cu 10% dan perlakuan sonikasi. Doping Cu mengurangi celah pita dan memperluas penyerapan cahaya ke daerah tampak, sementara $BiVO_4$ mendorong pemisahan muatan yang efektif. Analisis SEM-EDS mengungkapkan distribusi partikel yang lebih seragam dalam sampel yang disonikasi, dan UV-Vis DRS mengonfirmasi penyempitan celah pita yang substansial dari 2,97 eV menjadi 2,02 eV. Pengujian PEC dalam larutan NaCl 0,5 M menunjukkan bahwa komposit yang disonikasi mencapai tegangan foto tertinggi dan paling stabil (0,78 V) bersama dengan pembentukan gelembung hidrogen tampak, yang menunjukkan konversi cahaya menjadi hidrogen yang efisien. Temuan ini menunjukkan bahwa sonikasi memainkan peran penting dalam meningkatkan dispersi partikel, menekan penggumpalan, dan memperkuat heterojunction TiO_2/$BiVO_4$, yang menyoroti potensinya sebagai fotoanoda bias-sendiri untuk produksi hidrogen berkelanjutan.

* Corresponding author.
E-mail address: bunganurkhalifah03@gmail.com; vera.pangni@ft.unsika.ac.id

1. Introduction

The dwindling availability of fossil fuels, coupled with a surge in energy consumption due to population growth and industrialization, has been highlighted by Shiva Kumar & Himabindu (2019) and Anandha Priya et al. (2022) as the main causes of the global energy crisis. To address this challenge, the development of alternative energy sources has become critically important. Hydrogen, as highlighted by Yun et al. (2023), is an ideal clean energy source as it produces only water vapor without carbon emissions when used. (Yun et al., 2023) also note that 95% of global hydrogen is still produced through steam methane reforming (SMR), a method responsible for 76% of production and CO_2 emissions reaching 830 million tons in 2019 as a low-carbon solution (Shankar et al., 2023) explain that utilizing solar energy to split water into hydrogen mimics the process of photosynthesis and is a promising approach to energy conversion.

Photochemical water splitting has been recognized as a promising method for large-scale hydrogen production because it can use sunlight and photocatalysts to split water into H_2 and O_2 without greenhouse gas emissions (Guo et al., 2021; Kawawaki et al., 2021). Photoelectrochemical (PEC) technology offers a similar approach by utilizing semiconductor photoelectrodes to convert light energy into chemical energy (El-Shazly et al., 2021; Wang et al., 2021; Xia et al., 2024). The photoelectrocatalysis process is known to enhance the efficiency of reactive radical production through the synergy of photocatalytic and electrolytic processes, making PEC an efficient and economical solution for solar-based hydrogen production (Divyapriya et al., 2021; Shiva Kumar & Himabindu, 2019). It has been studied that efficiency remains low (<10%) due to degradation and photocorrosion of photoactive materials (Nabgan et al., 2024).

TiO_2 was first introduced as a photoelectrode by Fujishima and Honda in 1972 (Clark & Felsenfeld, 1972) and has continued to be used due to its stable, non-toxic, and corrosion-resistant properties (El-Shazly et al., 2021; Madkhali et al., 2023; Xia et al., 2024). The large band gap of TiO_2 (3.0–3.2 eV) limits its activity to UV light and causes high charge recombination (Eidsvåg et al., 2021; Ikreedeegh & Tahir, 2023; Moretti et al., 2021). Various modifications have been made, such as metal doping and composite formation (Asif Javed et al., 2021; Ikreedeegh & Tahir, 2023). Copper (Cu) is an excellent dopant because it can reduce the band gap, enhance visible light absorption, and improve charge separation efficiency at a low cost (Nankya & Kim, 2016; Tian et al., 2021; Yang et al., 2022). Additionally, $BiVO_4$ is promising due to its narrow bandgap (2.4 eV) and activity in visible light, although it is still constrained by charge transfer efficiency (Chen et al., 2020; Kamble et al., 2023; Nguyen et al., 2020).

The incorporation of TiO_2 and $BiVO_4$ into a heterojunction structure has been widely recognized as an effective approach to enhance photocatalytic efficiency through improved charge separation, extended light absorption, and the availability of more active reaction sites (Lv et al., 2019). In the $BiVO_4/TiO_2$ system, electrons migrate from the conduction band of $BiVO_4$ to TiO_2, while holes transfer from the valence band of TiO_2 to $BiVO_4$, thereby reducing charge recombination (Hu et al., 2020; Lv et al., 2019; Song, 2023). Nevertheless, an excessive proportion of $BiVO_4$ can diminish the active role of TiO_2 and result in economic inefficiency (Lv et al., 2019). To address this, Dozzi et al. (2016) suggested the use of metal doping, such as Cu, to improve charge transfer efficiency and increase the number of active sites. The Cu–TiO_2/$BiVO_4$ composite has therefore been considered highly promising for various photocatalytic applications, including water splitting, CO_2 reduction, and wastewater treatment. However, the Cu–TiO_2/$BiVO_4$ heterojunction composite remains relatively underexplored in the specific context of photoelectrochemical hydrogen production (Jabbari et al., 2024), providing a strong motivation for further study.

Previous investigations into Cu–TiO_2/$BiVO_4$ composites have primarily focused on doping and heterojunction design, but often overlooked critical challenges such as particle agglomeration and film instability, both of which limit long-term PEC performance. For instance, Jabbari et al. (2024) reported Cu–TiO_2/$BiVO_4$ composites with improved photocatalytic activity, yet their work did not address stability issues arising from particle agglomeration. In contrast, this study employs sonication as a novel strategy to suppress agglomeration and improve long-term PEC performance, thereby filling this gap and positioning sonication-assisted Cu–TiO_2/$BiVO_4$ as a unique contribution beyond existing studies. By combining 10% Cu doping, $BiVO_4$ coupling, and controlled sonication treatment, this study develops photocatalytic materials with improved homogeneity, reduced agglomeration, and uniform Cu dispersion in the TiO_2 matrix. These conditions are optimal for stabilizing the system before agglomeration occurs through Ostwald ripening (Kunzelmann et al., 2022; Mahdavi et al., 2022). The research systematically evaluates the effects of Cu doping, $BiVO_4$ heterojunction formation, and sonication treatment on morphology, optical properties, band gap narrowing, charge transfer efficiency, and PEC performance in 0.5 M NaCl electrolyte. By directly comparing pure TiO_2 with both sonicated and non-sonicated composites, this work demonstrates that sonication-assisted heterojunction engineering is an effective and innovative strategy to enhance structural stability and photoelectrochemical performance, offering valuable insights for the rational design of advanced photocatalysts in solar-driven water splitting.

2. Research Methods

This study utilized various laboratory equipment to support the synthesis and characterization of photocatalytic materials, including chemical glassware, beakers, dropper pipettes, stirring rods, spatulas, porcelain dishes, watch glasses, and digital balances. The dissolution and mixing processes were carried out using a hotplate with a magnetic stirrer, sonication using a sonicator, and drying using an oven. For film coating, ITO glass (2.5 × 1.25 cm), epoxy resin adhesive, and a spin coater were used. The photocatalytic process is supported by a 100-watt UV lamp in a photocatalytic box. Other auxiliary tools include a 450 mL glass compartment, copper (Cu) plates, 6 mm adapter connectors, alligator clips, a multimeter, paper tape, 2.5 mm copper wire, and 6 mm tubing. The chemicals used include Titanium Dioxide (TiO_2) as the base material, Copper (II) Acetate Monohydrate ($Cu(CH_3COO)_2$) as the dopant, Bismuth Nitrate Pentahydrate (98%), and Ammonium Metavanadate (99%) as precursors for $BiVO_4$. The solvents and stabilizing agents used include isopropanol, monoethanolamine (MEA), polyethylene glycol (PEG), and citric acid, while nitric acid (70%) and sodium hydroxide are used for pH adjustment. Additionally, NaCl, tap water, and deionized water are used for dissolution, washing, and cleaning during the process.

2.1 Preparation of Cu–TiO_2/$BiVO_4$ Anode

Material Cu–TiO_2 was synthesized using a sol-gel method by mixing 2.743 g of TiO_2 with 50 mL of isopropanol and stirring for 45 minutes. The Cu dopant was added in the form of Copper (II) Acetate Monohydrate at 0% and 10% of the TiO_2 weight, followed by further stirring. Subsequently, 1.4 mL of Monoethanolamine (MEA) was introduced as a stabilizing agent and stirred for 90 minutes until a stable sol was obtained, which was then left to stand overnight. On the following day, 4.42 mL of polyethylene glycol (PEG) was added to aid in particle texture formation (La Ode Asmin & Isa, 2020). Two variations were prepared: one without sonication and the other subjected to 10 minutes of ultrasonic treatment using an Ultrasonic Cleaner, a duration selected based on previous reports showing that short exposure (≤10 min) promotes homogeneous precursor mixing, suppresses agglomeration, and improves dopant incorporation, while longer treatment (>15 min) can destabilize sols and reduce material stability (Kunzelmann et al., 2022; Mahdavi et al., 2022). After sol–gel preparation, the solution was heated at 200 °C for 2 hours to evaporate the solvent, producing a Cu–TiO_2 paste that was deposited onto 2.5 × 1.25 cm ITO glass substrates using the doctor blade method (Davies et al., 2023). To ensure optimal crystallization and particle bonding, the drying and annealing process was repeated twice at 200 °C.

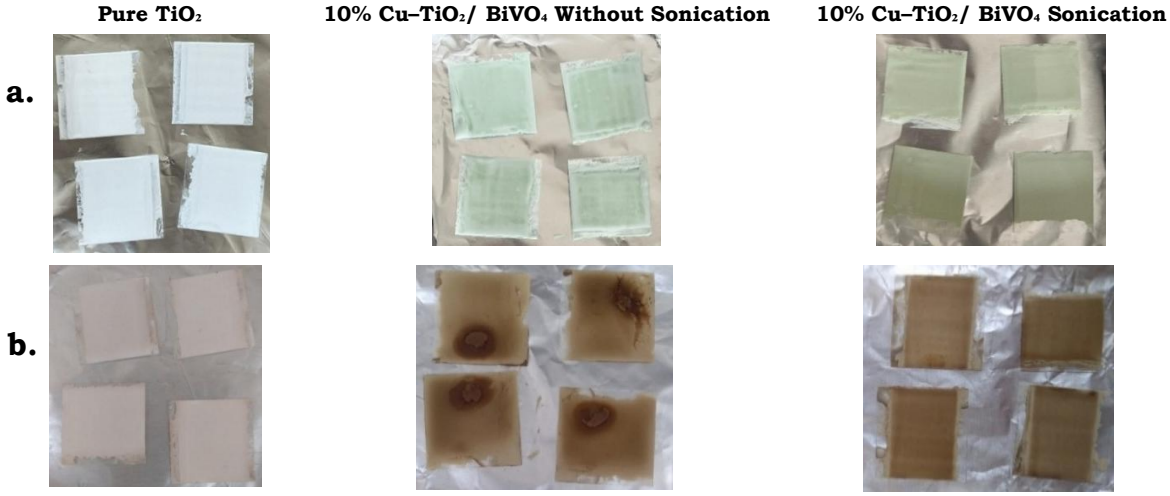

Figure 1. Glass coated with three types of photocatalyst materials, (a) before and (b) after the annealing process

During the coating and thermal treatment process, distinct color changes were observed (**Figure 1**), indicating the successful incorporation of Cu dopants and their influence on the material structure. Pure TiO_2 maintained its bright white color before and after annealing, confirming the structural stability of the anatase phase. In contrast, the 10% Cu–TiO_2 sample without sonication changed from light green to dark brown with uneven spots, suggesting pronounced Cu particle agglomeration. Meanwhile, the sonicated 10% Cu–TiO_2 sample exhibited a uniform golden-brown color, reflecting more homogeneous Cu dispersion within the TiO_2 matrix. These visual changes demonstrate structural modifications and Cu^{2+} ion interactions in the TiO_2 network, which play a critical role in determining the optical properties, electrical conductivity, and photocatalytic activity of the material (Davies et al., 2023; Nankya & Kim, 2016).

$BiVO_4$ was synthesized following a method adapted from Davies et al. (2023) and Choi et al. (2017), by dissolving NH_4VO_3, $Bi(NO_3)_3{\cdot}5H_2O$, citric acid, and HNO_3 in deionized water, followed by sonication. The resulting solution was deposited onto the Cu–TiO_2 surface using the spin-coating method and annealed at 250 °C to improve crystallinity and interfacial bonding. The photoanode was then assembled by attaching an insulated copper wire and sealing it with epoxy resin, leaving an active surface area of approximately 1.25 cm^2 to support the photoelectrochemical measurements (**Figure 2**).

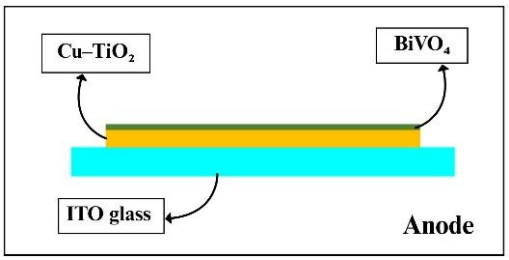

Figure 2. Illustration of the position of the layer above the ITO glass

The coating stage was carried out using the spin coating method on the Cu–TiO_2 surface to form a thin, even layer. The process began at a low speed of 300 RPM for 5 seconds for the initial spreading of the solution, then continued with an increase in speed to 1000 RPM for 10 seconds to obtain a more uniform layer. In this composite system, the ratio of Cu–TiO_2 is used in a larger amount compared to $BiVO_4$. After the coating process, the samples were annealed at 250°C with a heating time (ramp time) of 1 hour and a holding time of 2.5 hours to crystallize the

$BiVO_4$ structure and strengthen the integration between layers (Choi et al., 2017; Davies et al., 2023). As an electrical contact, an insulated copper wire that has been flattened is attached to the ITO glass area that is not coated with material. Next, the electrodes were coated with epoxy resin adhesive to prevent direct contact between the electrolyte and unwanted areas, leaving only an active area of approximately 1.25 cm^2, as shown in **Figure 3**. This area serves as the reactive surface in the photoelectrochemical system. This arrangement is designed to concentrate the photocatalytic reaction and enhance the efficiency of the PEC system.

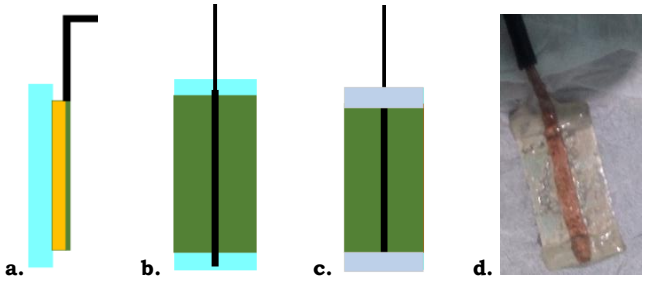

Figure 3. Installation of anode components: (a) Side view, (b) Front view, (c) Epoxy resin coating, and (d) Actual installation view

2.2 Cathode Preparation

The cathode preparation stage was carried out without any special modifications, using only a 2 cm wide and 1.5 mm thick copper plate and insulated copper wire as an electrical connector. Although simple, this stage is important to ensure the conductivity and stability of the cathode in the photoelectrochemical system.

2.3 Trial

The photoelectrochemical (PEC) experiments were conducted in a single-compartment glass cell (8 × 10 cm, maximum capacity 450 mL) with a modified lid to accommodate electrodes and gas circulation. The lid contained two small holes (0.5 cm) for wire connections and one larger hole (1.5 cm) for a gas adapter, ensuring stability and minimizing leakage. The electrode system consisted of an ITO glass anode coated with Cu–TiO_2/$BiVO_4$ and a copper (Cu) cathode, connected with insulated copper wires and sealed to prevent air leakage. The cell was filled with 400 mL of neutral electrolyte solution (pH 7) containing 0.5 M NaCl, prepared by dissolving 11.7 g NaCl according to the molarity equation. NaCl was selected not only for its neutrality and availability but also because chloride ions (Cl^-) can be activated to form reactive species such as ·Cl and ·ClO, which contribute to oxidation reactions while maintaining stable water oxidation pathways to O_2 (Zheng et al., 2021). Illumination was provided by a UV light source, and the intensity was calibrated with a lux meter prior to each test to ensure consistent irradiation conditions. The ITO/Cu–TiO_2/$BiVO_4$ photoanode (**Figure 4**) functions as a type-II heterojunction, where TiO_2 acts as the primary absorber and $BiVO_4$ serves as a surface modifier to enhance charge separation (Guan et al., 2021). Under illumination, electrons excited in $BiVO_4$ transfer to the TiO_2 conduction band and flow toward the Cu cathode, while photogenerated holes in $BiVO_4$ drive oxidation reactions. This heterojunction configuration suppresses electron–hole recombination, improves charge carrier lifetimes, and enhances overall energy conversion efficiency.

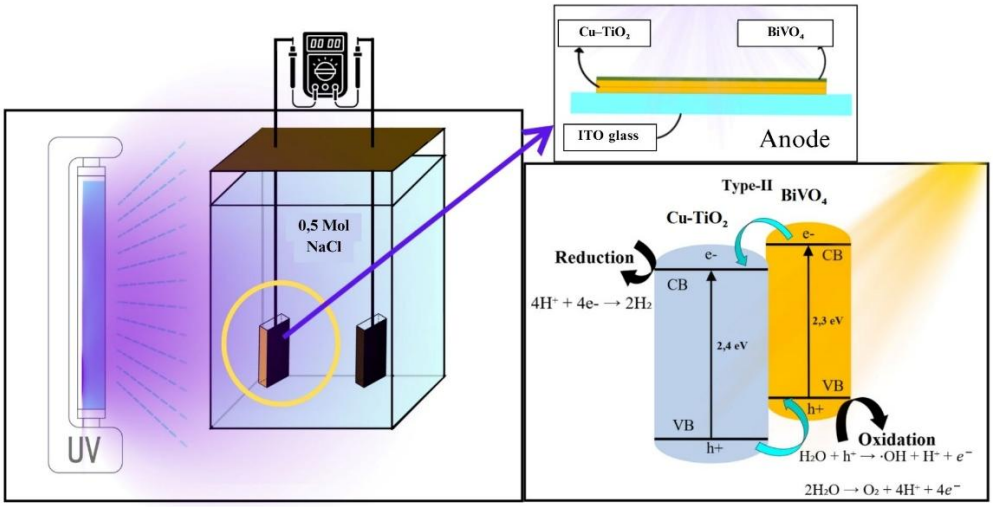

Figure 4. Photoelectrochemical (PEC) water splitting system with Cu–TiO_2/$BiVO_4$ in 1 compartment

To ensure reliability and reproducibility, replicate measurements were conducted following literature standards (Guan et al., 2021; Mahdavi et al., 2022). Three independent trials were performed for pure TiO_2 and the sonicated 10% Cu–TiO_2/$BiVO_4$ samples, while two trials were carried out for the non-sonicated composite due to lower film stability. The close overlap of voltage time curves across replicates, particularly for the sonicated samples, confirmed reproducibility and structural stability of the prepared electrodes. This systematic approach, combining calibrated illumination, controlled electrolyte composition, and replicated measurements, provides a robust experimental basis

for evaluating the role of Cu doping, $BiVO_4$ heterojunction formation, and sonication treatment in enhancing PEC performance.

2.4 Morphological Characterization

Characterization using Scanning Electron Microscopy (SEM) and Energy Dispersive X-ray Spectroscopy (EDS/EDAX) aims to analyze surface morphology, particle shape and distribution, and elemental composition in nanomaterials.

2.5 Band Gap Energy Analysis

The UV-Vis DRS (Diffuse Reflectance Spectroscopy) method is used to analyze light absorption and determine the band gap energy of photocatalytic semiconductor materials in photoelectrochemical (PEC) systems. Band gap calculations use the Tauc method, which is based on the relationship between the absorption coefficient (α), photon energy (hv), and type of electronic transition (γ), namely ½ for direct transitions and 2 for indirect transitions. Reflectance data is converted into absorption data using the Kubelka-Munk function ($F(R\infty)$) to enable the Tauc graphical approach in estimating the band gap value (Makuła et al., 2018).

The Tauc method is based on the assumption that the energy-dependent absorption coefficient (α) can be expressed through the following equation:

$$(\alpha.hv)^{1/y} = B(hv - E_g) \quad (1)$$

where h = Planck's constant, υ = photon frequency, Eg = band gap energy, B = a constant, and γ = depends on the nature of the electron transition: ½ for direct transitions and 2 for indirect transitions.

Munk (1931) proposed a method whereby the measured reflectance spectrum can be converted into a corresponding absorption spectrum by applying the Kubelka–Munk function.

$$(F(R\infty)) = \frac{K}{S} = \frac{(1-R)^2}{2R} \quad (2)$$

where ($F(R\infty)$)= Kubelka-Munk factor, K = Absorbance coefficient, S = Scattering coefficient and ($R\infty$) = Measured reflectance value. (Makuła et al., 2018)

The F value is related to photon energy through the equation:

$$(F(R\infty).hv)^{1/y} = B(hv - E_g) \quad (3)$$

3. Results and Discussion

This study discusses the improvement of the photoelectrochemical performance of TiO_2 material through the formation of Cu–TiO_2/$BiVO_4$ heterojunction composites with 10% Cu doping, as well as treatment with and without sonication. The addition of Cu dopant aims to reduce the band gap value and expand the light absorption spectrum to the visible region, while the addition of $BiVO_4$ serves to accelerate the charge separation process. The testing process was conducted using a single-compartment cell with a 0.5 Mol NaCl electrolyte solution as the reaction medium.

3.1 Morphological Analysis of Cu–TiO_2/$BiVO_4$

Morphological characterization of pure TiO_2 using SEM at 10,000× magnification revealed spherical particles with light agglomeration. This morphology is consistent with the literature by Lv et al. (2019), who reported similar particle shapes with dense and rough surfaces. The particle size ranged from 0.022 to 0.152 µm. The EDS spectrum showed the dominant presence of Ti (4.5 keV) and O (0.53 keV), with minor carbon contamination (0.28 keV), confirming the relative purity of the initial material (**Figure 5a**). SEM results for the 10% Cu–TiO_2/$BiVO_4$ composite show larger particles (0.020–0.217 µm), irregular shapes, and more pronounced agglomeration (**Figure 5b**), indicating the influence of Cu doping on particle growth and distribution during synthesis.

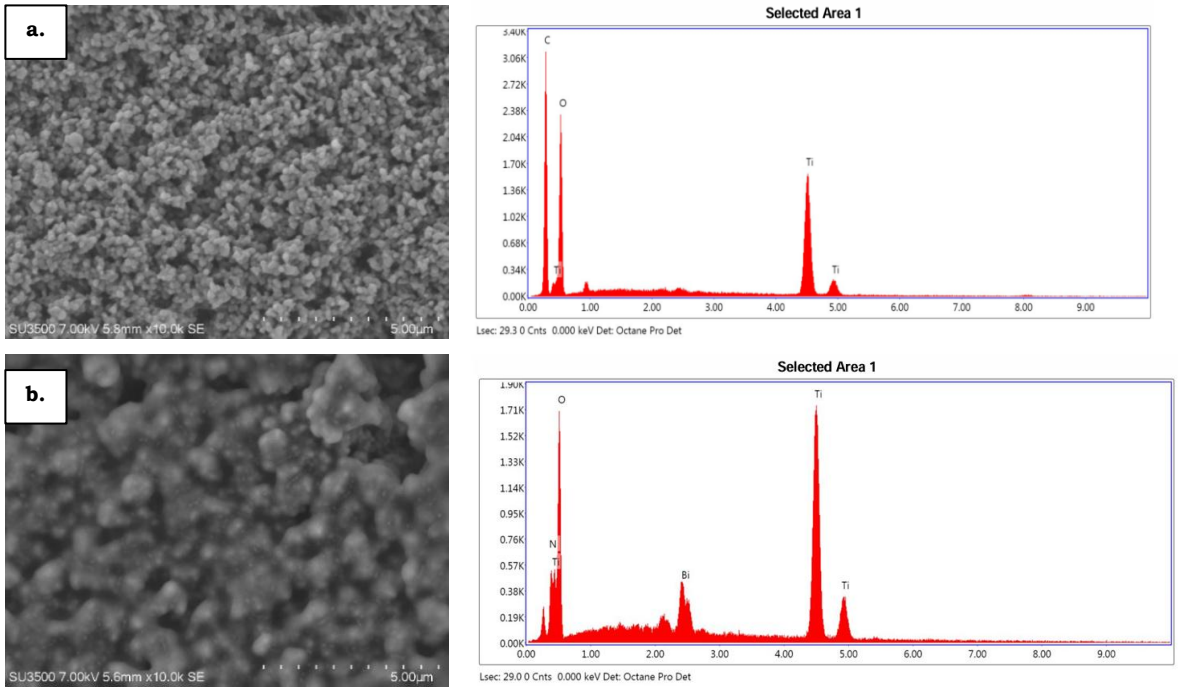

Figure 5. SEM and EDS spectrum test results: (a) Pure TiO_2, (b) 10% Cu–TiO_2/$BiVO_4$

In **Figure 5b**, the EDS spectra of the composite primarily display dominant Ti and O peaks, along with minor signals from bismuth (2.4 keV) and nitrogen (0.4 keV). The Cu peak is not observed, which may be attributed to its relatively low concentration (10% doping) and homogeneous incorporation within the TiO_2 lattice, leading to a signal that is overshadowed by the more intense Ti and O peaks. Similarly, the vanadium peak is absent, which could be explained by its very low concentration, possible uneven distribution within the $BiVO_4$ phase, or the intrinsic limitations of the EDS technique. Since EDS is semi-quantitative and primarily sensitive to elements above ~0.1 wt%, it is likely that the signals of Cu and V fall below its detection threshold. Furthermore, as EDS analyzes only localized surface areas, the probability of missing weak signals is increased if the elements are not uniformly distributed or are masked by dominant matrix elements.

To more conclusively verify the incorporation of Cu and V, complementary characterization techniques are strongly recommended. X-ray Photoelectron Spectroscopy (XPS) can provide high sensitivity to surface composition and oxidation states, offering direct evidence for Cu^{2+} and V^{5+} in the heterojunction. X-ray Diffraction (XRD) can confirm the crystalline phases of CuO, Cu_2O, or $BiVO_4$, thereby supporting indirect evidence of Cu and V integration, while Inductively Coupled Plasma (ICP-OES or ICP-MS) can deliver precise quantitative data even for trace-level elements beyond the detection limit of EDS. Although such advanced analyses were not conducted in the present study, they remain an important recommendation for future work, enabling a more comprehensive understanding and definitive confirmation of Cu and V incorporation in Cu–TiO_2/$BiVO_4$ heterojunction photocatalysts.

3.2 Optical Properties and Band Gap Analysis

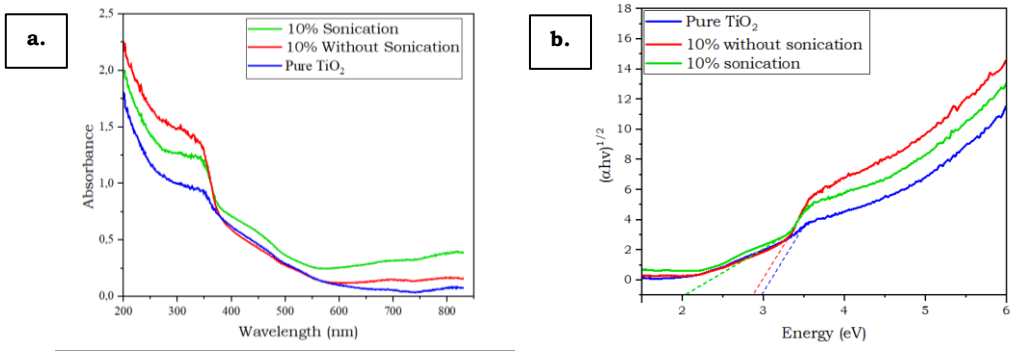

Figure 6. (a) UV–Vis DRS absorption spectrum and (b) Tauc curve for estimating the band gap energy of pure TiO_2, 10% Cu–TiO_2/$BiVO_4$ without sonication, and 10% Cu–TiO_2/$BiVO_4$ sonication

The UV-Vis DRS results (**Figure 6**) demonstrate that the introduction of 10% Cu doping, $BiVO_4$ heterojunction formation, and sonication treatment significantly influence the optical properties of Cu–TiO_2/$BiVO_4$ composites. Pure TiO_2 exhibits a band gap of 2.97 eV, characteristic of the anatase phase that is active mainly in the UV region, thereby limiting solar light utilization. The incorporation of $BiVO_4$ extends the absorption edge to 800 nm, confirming improved visible light harvesting. The Cu–TiO_2/$BiVO_4$ composite without sonication shows a moderate band gap reduction to 2.86 eV, reflecting partial electronic interaction but still constrained by particle agglomeration and

suboptimal band alignment. In contrast, the sonicated Cu–TiO_2/$BiVO_4$ composite exhibits a substantial band gap reduction to 2.02 eV, shifting the absorption edge into the visible-light region (600 nm). This pronounced improvement is attributed to the enhanced particle dispersion, suppression of agglomeration, and the formation of more effective type II heterojunctions induced by ultrasonic treatment, which facilitate spatial charge separation, extend charge carrier lifetimes, and minimize recombination losses. These findings are consistent with Jabbari et al. (2024), who similarly reported that heterojunction engineering and band structure modification significantly enhance light absorption and photocatalytic activity in Cu–TiO_2/$BiVO_4$ systems.

Although the band gap values reported in this study are based on qualitative estimation without error margins or statistical analysis, the consistent trend observed across all samples strongly confirms the beneficial role of sonication in tailoring the optical properties of Cu–TiO_2/$BiVO_4$ composites. The broadened absorption spectrum in the lower-energy region and the increased visible-light response in the sonicated samples clearly demonstrate enhanced excitation efficiency and more favorable charge carrier dynamics, reinforcing their potential for visible light-driven applications. Taken together, these findings establish sonication as an effective modification strategy that not only reduces the band gap into the optimal range for visible-light absorption (2.0–2.8 eV) but also strengthens heterojunction interfaces, thereby positioning Cu–TiO_2/$BiVO_4$ as a promising candidate for solar-driven photocatalytic applications. To further substantiate these results, future studies are recommended to include statistical validation and error analysis, providing a more quantitative assessment of band gap tuning and photocatalytic efficiency.

3.3 Electricity Production Prospects

The products generated by the photoelectrochemical system are not limited to hydrogen gas. The detection of hydrogen gas generally requires instruments such as a gas chromatograph or an eudiometer. This system can also generate electrical energy directly through light-induced electron excitation, which can be measured using a multimeter. **Figure 4** shows the system used to test the ability of the Cu–TiO_2/$BiVO_4$ composite material to convert light energy into electrical energy. The photoanode structure comprises ITO/Cu–TiO_2/$BiVO_4$ glass, with the $BiVO_4$ layer acting as the primary light absorber (**Figure 2**), while the thicker Cu–TiO_2 layer acts as an additional absorber and forms a type II heterojunction to facilitate charge separation. When exposed to UV-Vis light, photons induce electron excitation from the valence band to the conduction band of $BiVO_4$. These electrons then transfer to the conduction band of the Cu–TiO_2 layer, while holes remain in the $BiVO_4$ layer to facilitate oxidation reactions (Guan et al., 2021). The separated electrons are transferred to the ITO glass and passed to the copper cathode via an external circuit, producing an electric current that can be measured using a multimeter. In this system, a 0.5 molar solution of sodium chloride (NaCl) enhances conductivity and facilitates charge transfer between the electrodes. Although Cl^- ions in the solution have the potential to oxidise to form chlorine gas, the evolution of O_2 from water remains dominant due to the high oxidation capacity of $BiVO_4$ (Zheng et al., 2021). The enhanced charge separation efficiency achieved through the formation of this type II heterojunction prevents electron-hole pair recombination. This allows redox reactions to proceed optimally and improves the efficiency of the photoelectrochemical system, making it similar to light-driven electrolysis processes.

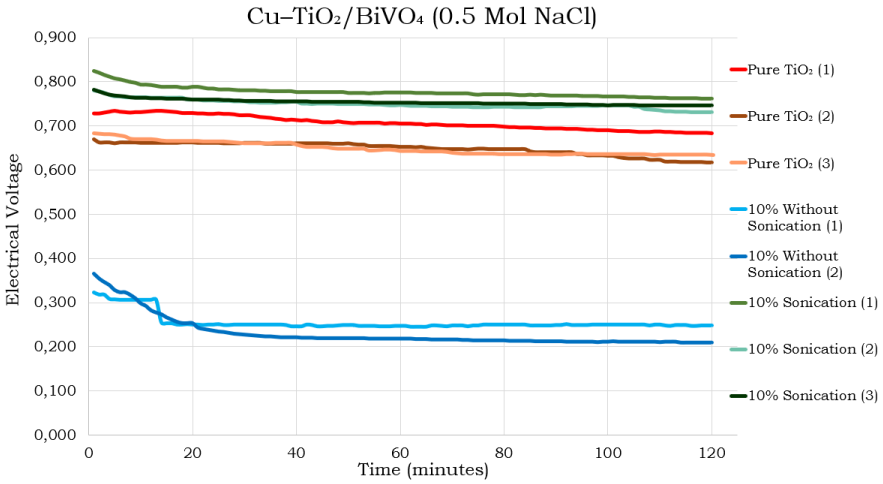

Figure 7. Graph of Electrical Voltage Resulting from Photocatalytic Reaction

The photoelectrocatalytic (PEC) results (**Figure 7**) demonstrate that the sonicated 10% Cu–TiO_2/$BiVO_4$ composite achieved the highest performance, reaching an initial voltage of 0.77–0.82 V that stabilized at 0.76–0.78 V after 120 minutes. This improvement reflects the role of sonication in enhancing Cu dopant dispersion, reducing agglomeration, and promoting robust type-II heterojunction formation, thereby suppressing charge recombination and strengthening interfacial bonding to the ITO substrate, consistent with the principles highlighted by Hu et al. (2020). Meanwhile, **Table 1** shows that pure TiO_2 stabilized at 0.62–0.68 V, whereas the non-sonicated composite declined markedly from 0.32 V to 0.22–0.25 V. Although the enhancement over pure TiO_2 (0.73 → 0.76–0.78 V) may appear modest, the absence of overlap between the stable ranges provides clear statistical evidence of systematic improvement. Collectively, these results confirm that sonication is a decisive factor in reinforcing structural integrity and sustaining PEC efficiency during long-term operation.

Table 1. Electrical Production Performance of Cu–TiO_2/$BiVO_4$ Material

Sample	Time (Minutes)	Electrical Voltage (V)	Electrical Voltage (V)
		First	Stable
Pure TiO_2	120	0.73–0.67	0.62–0.68
10% Cu–TiO_2/$BiVO_4$ Without Sonication	120	0.32	0.22–0.25
10% Cu–TiO_2/$BiVO_4$ Sonication	120	0.82	0.76–0.78

For comparison, Jiang et al. (2018) reported TiO_2/$BiVO_4$ photoanodes requiring an external bias of 1.0–1.2 V vs. RHE to achieve stable operation, while Resasco et al. (2016) achieved only ~0.6 V under similar conditions. In contrast, the present system operates effectively at 0.78 V without external bias and remains stable for more than 120 minutes, demonstrating a competitive and practical advantage. Furthermore, the 0.45–0.5 V improvement compared to the non-sonicated counterpart provides quantitative confirmation that ultrasonic treatment is critical for enhancing structural stability and PEC activity. This observation is consistent with Mahdavi et al. (2022) and other $BiVO_4$-based sonication studies, which report that ultrasonic processing improves particle dispersion, suppresses agglomeration, and produces more durable photoelectrodes. Optical characterization further substantiates these findings, showing that band gap narrowing from 2.97 eV (pure TiO_2) to 2.02 eV (sonicated Cu–TiO_2/$BiVO_4$) extends absorption into the visible-light region (up to 600 nm), thereby increasing photon utilization and excitation efficiency. Sonication promotes homogeneous mixing, uniform dopant incorporation, and stronger interfacial bonding between TiO_2 and $BiVO_4$, which collectively enhance charge separation and prolong carrier lifetimes (Wu et al., 2022). Taken together, these results firmly establish the sonication-assisted Cu–TiO_2/$BiVO_4$ composite as a promising self-biased photoanode capable of stable low voltage operation, offering performance that rivals or surpasses many externally biased systems.

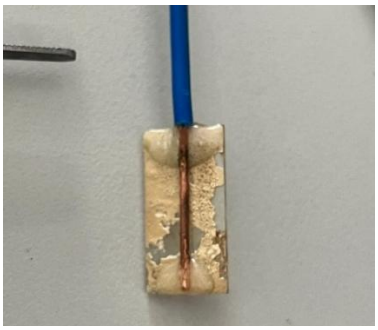

Figure 8. Condition of 10% Cu-TiO_2/$BiVO_4$ electrode without sonication after photocatalytic testing, showing the release of the layer from the ITO glass substrate

Conversely, the non-sonicated 10% Cu–TiO_2/$BiVO_4$ composite exhibited the weakest PEC performance, starting at only 0.32 V and declining to a stable range of 0.22–0.25 V after 120 minutes (**Table 1**). This severe deterioration was accompanied by poor adhesion of the composite layer to the ITO substrate, as evidenced by peeling in **Figure 8**, indicating low structural integrity and unstable electrochemical behavior. Such degradation is consistent with previous observations that inadequate dispersion of dopants leads to particle agglomeration, creating recombination centers and reducing the effective surface area available for redox reactions (Mahdavi et al., 2022). Interestingly, pure TiO_2, despite its wider band gap (2.97 eV) and limited visible-light absorption, maintained a relatively higher and more stable output (0.73–0.67 V initially, stabilizing at 0.68–0.62 V) compared to the non-sonicated composite, demonstrating that improper dopant incorporation can be more detrimental than the absence of doping. In contrast, the sonicated 10% Cu–TiO_2/$BiVO_4$ composite achieved the best performance, with an initial voltage of 0.82 V that stabilized at 0.76–0.78 V, underscoring that sonication is not a trivial modification but a decisive strategy for achieving homogeneous dopant distribution, robust heterojunction formation, and durable PEC operation findings that align with prior reports on sonication-enhanced heterojunction systems(Mahdavi et al., 2022; Wu et al., 2022).

4. Conclusion

This study demonstrates that while 10% Cu doping in TiO_2 enhances heterojunction formation, it also promotes particle agglomeration and compromises stability when applied without further modification. The introduction of sonication emerges as the decisive factor that overcomes these limitations by enabling homogeneous particle dispersion, suppressing agglomeration, and facilitating the formation of robust type-II heterojunctions with $BiVO_4$. As a result, the sonicated Cu–TiO_2/$BiVO_4$ composite exhibited substantial band gap narrowing from 2.97 eV to 2.02 eV, improved visible-light absorption, and the highest PEC performance (0.82 → 0.76–0.78 V) with excellent stability, clearly outperforming both pure TiO_2 and non-sonicated composites. These findings highlight sonication not only as a synthesis aid but as a key innovation that enhances structural stability, charge transfer efficiency, and photocatalytic activity. More broadly, this work positions sonication-assisted Cu–TiO_2/$BiVO_4$ as a promising self-biased photoanode for solar-driven water splitting and suggests that sonication-based modification strategies hold strong potential for the future development of efficient PEC materials.

5. References

Anandha Priya, B., Sivakumar, T., & Venkateswari, P. (2022). Construction of MoS2 nanoparticles incorporated TiO2 nanosheets heterojunction photocatalyst for enhanced visible light driven hydrogen production. *Inorganic*

Chemistry Communications, *136*(December 2021), 109118. https://doi.org/10.1016/j.inoche.2021.109118

Asif Javed, H. M., Qureshi, A. A., Mehmood, R., Tahir, M. I., Javed, S., Sarfaraz, M., Javaid, M. Y., Awais, M., & Ali, U. (2021). Hydrogen treated TiO2 nanoparticles onto FTO glass as photoanode for dye-sensitized solar cells with remarkably enhanced performance. *International Journal of Hydrogen Energy*, *46*(27), 14311–14321. https://doi.org/10.1016/j.ijhydene.2021.01.184

Chen, S. H., Jiang, Y. S., & Lin, H. Y. (2020). Easy Synthesis of BiVO4 for Photocatalytic Overall Water Splitting. *ACS Omega*, *5*(15), 8927–8933. https://doi.org/10.1021/acsomega.0c00699

Choi, J., Sudhagar, P., Kim, J. H., Kwon, J., Kim, J., Terashima, C., Fujishima, A., Song, T., & Paik, U. (2017). WO3/W:BiVO4/BiVO4 graded photoabsorber electrode for enhanced photoelectrocatalytic solar light driven water oxidation. *Physical Chemistry Chemical Physics*, *19*(6), 4648–4655. https://doi.org/10.1039/c6cp08199a

Clark, R. J., & Felsenfeld, G. (1972). © 1972 Nature Publishing Group. *Nature New Biology*, *240*, 226–229. https://doi.org/10.1038/239137a0

Davies, K. R., Allan, M. G., Nagarajan, S., Townsend, R., Dunlop, T., McGettrick, J. D., Asokan, V. S., Ananthraj, S., Watson, T., Godfrey, A. R., Durrant, J. R., Maroto-Valer, M. M., Kuehnel, M. F., & Pitchaimuthu, S. (2023). Solar light-driven simultaneous pharmaceutical pollutant degradation and green hydrogen production using a mesoporous nanoscale WO3/BiVO4 heterostructure photoanode. *Journal of Environmental Chemical Engineering*, *11*(3), 110256. https://doi.org/10.1016/j.jece.2023.110256

Divyapriya, G., Singh, S., Martínez-Huitle, C. A., Scaria, J., Karim, A. V., & Nidheesh, P. V. (2021). Treatment of real wastewater by photoelectrochemical methods: An overview. *Chemosphere*, *276*, 130188. https://doi.org/10.1016/j.chemosphere.2021.130188

Dozzi, M. V., Marzorati, S., Longhi, M., Coduri, M., Artiglia, L., & Selli, E. (2016). Photocatalytic activity of TiO2-WO3 mixed oxides in relation to electron transfer efficiency. *Applied Catalysis B: Environmental*, *186*, 157–165. https://doi.org/10.1016/j.apcatb.2016.01.004

Eidsvåg, H., Bentouba, S., Vajeeston, P., Yohi, S., & Velauthapillai, D. (2021). Tio2 as a photocatalyst for water splitting—an experimental and theoretical review. *Molecules*, *26*(6), 1–30. https://doi.org/10.3390/molecules26061687

El-Shazly, A. N., Hegazy, A. H., El Shenawy, E. T., Hamza, M. A., & Allam, N. K. (2021). Novel facet-engineered multi-doped TiO2 mesocrystals with unprecedented visible light photocatalytic hydrogen production. *Solar Energy Materials and Solar Cells*, *220*(October 2020), 110825. https://doi.org/10.1016/j.solmat.2020.110825

Guan, Y., Liu, Y., Lv, Q., & Wu, J. (2021). Bismuth-based photocatalyst for photocatalytic oxidation of flue gas mercury removal: A review. *Journal of Hazardous Materials*, *418*(28), 126280. https://doi.org/10.1016/j.jhazmat.2021.126280

Guo, S., Li, X., Li, J., & Wei, B. (2021). Boosting photocatalytic hydrogen production from water by photothermally induced biphase systems. *Nature Communications*, *12*(1), 1–10. https://doi.org/10.1038/s41467-021-21526-4

Hu, K., E, L., Li, Y., Zhao, X., Zhao, D., Zhao, W., & Rong, H. (2020). Photocatalytic Degradation Mechanism of the Visible-Light Responsive BiVO4/TiO2 Core–Shell Heterojunction Photocatalyst. *Journal of Inorganic and Organometallic Polymers and Materials*, *30*(3), 775–788. https://doi.org/10.1007/s10904-019-01217-w

Ikreedeegh, R. R., & Tahir, M. (2023). Ternary nanocomposite of NH2-MIL-125(Ti) MOF-modified TiO2 nanotube arrays (TNTs) with GO electron mediator for enhanced photocatalytic conversion of CO2 to solar fuels under visible light. *Journal of Alloys and Compounds*, *969*(February), 172465. https://doi.org/10.1016/j.jallcom.2023.172465

Jabbari, P., Najafi Chermahini, A., Luque, R., Pineda, A., & Castellón, E. R. (2024). Synthesis of Cu-doped TiO2 modified BiVO4 for photocatalytic oxidative desulfurization (PODS) of a model fuel. *Journal of Photochemistry and Photobiology A: Chemistry*, *452*(January), 1–10. https://doi.org/10.1016/j.jphotochem.2024.115625

Jiang, W., Jiang, Y., Tong, J., Zhang, Q., Li, S., Tong, H., & Xia, L. (2018). Efficient photoelectrochemical water oxidation using a TiO 2 nanosphere-decorated BiVO 4 heterojunction photoanode. *RSC Advances*, *8*(72), 41439–41444. https://doi.org/10.1039/c8ra09072f

Kamble, G. S., Natarajan, T. S., Patil, S. S., Thomas, M., Chougale, R. K., Sanadi, P. D., Siddharth, U. S., & Ling, Y. C. (2023). BiVO4 As a Sustainable and Emerging Photocatalyst: Synthesis Methodologies, Engineering Properties, and Its Volatile Organic Compounds Degradation Efficiency. *Nanomaterials*, *13*(9).

https://doi.org/10.3390/nano13091528

Kawawaki, T., Kataoka, Y., Ozaki, S., Kawachi, M., Hirata, M., & Negishi, Y. (2021). Creation of active water-splitting photocatalysts by controlling cocatalysts using atomically precise metal nanoclusters. *Chemical Communications*, *57*(4), 417–440. https://doi.org/10.1039/d0cc06809h

Kunzelmann, V. F., Jiang, C. M., Ihrke, I., Sirotti, E., Rieth, T., Henning, A., Eichhorn, J., & Sharp, I. D. (2022). Solution-based synthesis of wafer-scale epitaxial BiVO4 thin films exhibiting high structural and optoelectronic quality. *Journal of Materials Chemistry A*, *10*(22), 12026–12034. https://doi.org/10.1039/d1ta10732a

La Ode Asmin, & Isa, L. (2020). Synthesis and Characterization of Structural Nanocomposite Titanium Dioxide Copper-Doped Using the Impregnation Method. *Spektra: Jurnal Fisika Dan Aplikasinya*, *5*(1), 21–30. https://doi.org/10.21009/spektra.051.03

Lv, Y. R., Liu, C. J., He, R. K., Li, X., & Xu, Y. H. (2019). BiVO4/TiO2 heterojunction with enhanced photocatalytic activities and photoelectochemistry performances under visible light illumination. *Materials Research Bulletin*, *117*(January), 35–40. https://doi.org/10.1016/j.materresbull.2019.04.032

Madkhali, N., Prasad, C., Malkappa, K., Choi, H. Y., Govinda, V., Bahadur, I., & Abumousa, R. A. (2023). Recent update on photocatalytic degradation of pollutants in waste water using TiO2-based heterostructured materials. *Results in Engineering*, *17*(October 2022), 100920. https://doi.org/10.1016/j.rineng.2023.100920

Mahdavi, K., Zinatloo-Ajabshir, S., Yousif, Q. A., & Salavati-Niasari, M. (2022). Enhanced photocatalytic degradation of toxic contaminants using Dy2O3-SiO2 ceramic nanostructured materials fabricated by a new, simple and rapid sonochemical approach. *Ultrasonics Sonochemistry*, *82*(December 2021), 105892. https://doi.org/10.1016/j.ultsonch.2021.105892

Makuła, P., Pacia, M., & Macyk, W. (2018). How To Correctly Determine the Band Gap Energy of Modified Semiconductor Photocatalysts Based on UV-Vis Spectra. *Journal of Physical Chemistry Letters*, *9*(23), 6814–6817. https://doi.org/10.1021/acs.jpclett.8b02892

Moretti, E., Cattaruzza, E., Flora, C., Talon, A., Casini, E., & Vomiero, A. (2021). Photocatalytic performance of Cu-doped titania thin films under UV light irradiation. *Applied Surface Science*, *553*(March), 149535. https://doi.org/10.1016/j.apsusc.2021.149535

Nabgan, W., Nabgan, B., Jalil, A. A., Ikram, M., Hussain, I., Bahari, M. B., Tran, T. V., Alhassan, M., Owgi, A. H. K., Parashuram, L., Nordin, A. H., & Medina, F. (2024). A bibliometric examination and state-of-the-art overview of hydrogen generation from photoelectrochemical water splitting. *International Journal of Hydrogen Energy*, *52*, 358–380. https://doi.org/10.1016/j.ijhydene.2023.05.162

Nankya, R., & Kim, K. N. (2016). Sol-gel synthesis and characterization of Cu-TiO2 nanoparticles with enhanced optical and photocatalytic properties. *Journal of Nanoscience and Nanotechnology*, *16*(11), 11631–11634. https://doi.org/10.1166/jnn.2016.13564

Nguyen, T. D., Nguyen, V. H., Nanda, S., Vo, D. V. N., Nguyen, V. H., Van Tran, T., Nong, L. X., Nguyen, T. T., Bach, L. G., Abdullah, B., Hong, S. S., & Van Nguyen, T. (2020). BiVO4 photocatalysis design and applications to oxygen production and degradation of organic compounds: a review. *Environmental Chemistry Letters*, *18*(6), 1779–1801. https://doi.org/10.1007/s10311-020-01039-0

Resasco, J., Zhang, H., Kornienko, N., Becknell, N., Lee, H., Guo, J., Briseno, A. L., & Yang, P. (2016). TiO2/BiVO4 nanowire heterostructure photoanodes based on type II band alignment. *ACS Central Science*, *2*(2), 80–88. https://doi.org/10.1021/acscentsci.5b00402

Shankar, V., Dharani, S. P., Ravi, A., & SaravanaVadivu, A. (2023). A concise review: MXene-based photo catalytic and photo electrochemical water splitting reactions for the production of hydrogen. *International Journal of Hydrogen Energy*, *48*(57), 21654–21673. https://doi.org/10.1016/j.ijhydene.2023.03.031

Shiva Kumar, S., & Himabindu, V. (2019). Hydrogen production by PEM water electrolysis – A review. *Materials Science for Energy Technologies*, *2*(3), 442–454. https://doi.org/10.1016/j.mset.2019.03.002

Song, C. (2023). Enhancing photocatalytic degradation of hydrolyzed polyacrylamide in oilfield wastewater using BiVO4/TiO2 heterostructure nano-photocatalyst under visible light irradiation. *International Journal of Electrochemical Science*, *18*(12), 100363. https://doi.org/10.1016/J.IJOES.2023.100363

Tian, L., Li, Z., Xu, X., & Zhang, C. (2021). Advances in noble metal (Ru, Rh, and Ir) doping for boosting water splitting electrocatalysis. *Journal of Materials Chemistry A*, *9*(23), 13459–13470. https://doi.org/10.1039/d1ta01108a

Wang, Y., Wang, W., Fu, J., Liang, Y., Yao, L., & Zhu, T. (2021). Integrating the plasmonic sensitizer and electron relay into ZnO/Au/CdS sandwich nanotube array photoanode for efficient solar-to-hydrogen conversion with 3.2% efficiency. *Renewable Energy*, *168*, 647–658. https://doi.org/10.1016/j.renene.2020.12.076

Wu, H., Zhang, L., Du, A., Irani, R., van de Krol, R., Abdi, F. F., & Ng, Y. H. (2022). Low-bias photoelectrochemical water splitting via mediating trap states and small polaron hopping. *Nature Communications*, *13*(1), 1–12. https://doi.org/10.1038/s41467-022-33905-6

Xia, L., Sun, Y., Wang, Y., Yao, W., Wu, Q., Min, Y., & Xu, Q. (2024). Three dimensional nickel foam carried sea urchin-like copper-cobalt-cerium cathode for enhanced tetracycline wastewater purification in photocatalytic fuel cell. *Journal of Colloid and Interface Science*, *653*(PB), 1444–1454. https://doi.org/10.1016/j.jcis.2023.10.007

Yang, H., Wang, W., Wu, X., Siddique, M. S., Su, Z., Liu, M., & Yu, W. (2022). Reducing ROS generation and accelerating the photocatalytic degradation rate of PPCPs at neutral pH by doping Fe-N-C to g-C3N4. *Applied Catalysis B: Environmental*, *301*(September 2021), 120790. https://doi.org/10.1016/j.apcatb.2021.120790

Yun, S., Lee, J., Cho, H., & Kim, J. (2023). Oxy-fuel combustion-based blue hydrogen production with the integration of water electrolysis. *Energy Conversion and Management*, *291*(April), 117275. https://doi.org/10.1016/j.enconman.2023.117275

Zheng, Z., Ng, Y. H., Tang, Y., Li, Y., Chen, W., Wang, J., Li, X., & Li, L. (2021). Visible-light-driven photoelectrocatalytic activation of chloride by nanoporous MoS2@BiVO4 photoanode for enhanced degradation of bisphenol A. *Chemosphere*, *263*, 128279. https://doi.org/10.1016/j.chemosphere.2020.128279